Investigation of Water Injection Benefits on Downsized Boosted Direct Injection Spark Ignition Engine

Yuan ZHUANG[1], Yu SUN[1], Yuhan HUANG[3], Qin TENG[1], Bo HE[2], Wei CHENG[2], Yejian QIAN[1*]

[1] School of Automotive and Transportation Engineering, Hefei University of Technology, Hefei, China

[2] Anhui Jianghuai Automobile Group LTD Technical Center, Hefei, China

[3] Centre for Green Technology, School of Civil and Environmental Engineering, University of Technology Sydney, NSW 2007, Australia

[*] Corresponding author: Yejian QIAN, Email: xjwei@ustc.edu.cn

Abstract

Engine downsizing and boosting are key technologies to achieve the increasingly stringent emissions standards for spark ignition (SI) engines. However, knock is a major obstacle inhibiting further downsizing of SI engines. Water injection is a promising technology that has regained attention recently to solve the knock problem. In this paper, a 1.5L turbocharged gasoline direct injection (GDI) engine was modified by installing a water port injection (WPI) system on the intake manifold. The WPI system was modified from a GDI system and deionized water was pressured to 50 bar in a water tank by compressed nitrogen. The effect of WPI on engine combustion and emissions performance were experimentally investigated under different water/gasoline volume percentages and WPI timings. The results show that WPI has great potential in suppressing engine knock. At original engine setting (without adjustment of spark timing), all the combustion indexes related to knock are decreased by WPI, including maximum in-cylinder pressure (P_{max}) and maximum pressure rise rate (R_{max}). The flame kernel formation process (CA0-5), initiation combustion duration (CA0-10), early combustion duration (CA0-50) and major combustion duration (CA0-90) are deteriorated, resulting in decreased indicated mean effective pressure (IMEP) and thermal efficiency. By properly advancing spark timing, the combustion process can be improved, allowing the engine to achieve higher P_{max} and better combustion phases without occurrence of knock. It is also found that the water/gasoline volume percentage should be kept within a proper range (30% in this study) because over WPI can lead to deterioration of combustion and pollutant emissions. WPI can effectively reduce the production of NO and CO emissions, while HC emissions are increased with the rise of water/gasoline volume percentage.

Abbreviations

GDI	Gasoline direct injection	CA	Crank angle
WPI	Water port injection	BTDC	Before top dead center
FSN	Filter smoke number	ATDC	After top dead center
SI	Spark ignition	ECU	Electronic control unit
CO	Carbon monoxide	NO_X	Oxides of nitrogen
HC	Hydrocarbon	NO	Nitric oxide
PFI	Port fuel injection	PPM	Parts per million
DI	Direct injection	IMEP	Indicated mean effective pressure
MBT	Maximum brake torque	TDC	Top dead center
KLSA	Knock limited spark advance	ER	Equivalence ratio
IVC	Inlet valve closing	PI	Port injection

1. Introduction

Recently, downsized boosted spark ignition (SI) technology is progressing rapidly due to its potential in further conserving petroleum reserves and meeting increasingly stringent emissions standards [1,2]. Most world major automotive manufacturers have launched their downsized boosted SI engines and equipped them on their products. However, for downsized boosted engines, most of their operation ranges are in high indicated mean effective pressure (IMEP) range, resulting in high in-cylinder pressure and temperature and vulnerably leading to increased possibility of abnormal combustion events like knock, pre-ignition or even super-knock. Thus, the boost pressure and compression ratio in those engines have to be restricted, which in-turn limits the further increase of engine power density. Normally, retarded spark timing and mixture enrichment are applied to inhibit knock propensity, which compromise the thermal efficiency. To avoid using spark retard and mixture enrichment while to suppress knock at the same time, water injection technology has regained attention.

Water injection technology on boosted SI engines is not new. Hopkinson [3] proposed water injection as an internal coolant of gas engines in as early as 1913. The study of water injection's potential on knock mitigation could be traced back to early 1930s when Richard first tested its effect on a supercharged SI engine with compression of 7:1 [4]. During World War II, water injection was extensively used on aircraft mostly to boost the thrust during take-off. In the 1940s NACA (the predecessor to NASA) reported extensively on water injection experiments. Their studies showed that water injection had a marked cooling effect. An increase in the coolant-fuel ratio from 0.2 to 0.4 was 2.5 times as effective in raising the knock-limited IMEP. Water injection allowed an engine to be operated at a higher IMEP, with a lower indicated specific fuel consumption. In 1962, GM even launched a turbo car which had water injection fitted as standard – the 1962 Oldsmobile Jetfire Turbo Rocket. However, in the next few decades, the interests in water injection disappeared because of the advent of intercooler which could effectively cool the fresh charge and reduce the complexity of adding another injection system for water. The potential gain of water injection on engine efficiency has been investigated in recent years due to the imperative need of developing new generation of downsized boosted SI engine with specific power output around or above 110 kW/L and meet the latest emissions standards.

Currently, there are three strategies for water injection into engines, namely direct injection (DI) of water-fuel emulsion, water injection into the intake manifold (or fumigation), and direct water injection into combustion chamber. The strategies differ by increasing complexity and cost of the injection system and decreasing water consumption [5]. Injecting water-fuel emulsion into the cylinder through the original DI system requires a few or even no modifications for the engine. Water-fuel emulsion can be

generated off-board or on-board before injector or even in the injector itself [6,7]. Surfactants are used to decrease the surface tension of water and stabilize the water-fuel mixture. Thus, much consideration of this technology is put into the development of surfactants and generation of the emulsion. Direct water injection can make the best use of the great heat of vaporization of water to lower in-cylinder temperature and suppress knock. It also provides more flexibilities as DI timing and pressure can be actively controlled according to the engine needs. However, direct water injection requires two separates higher-pressure fuel systems and an extra injector to be mounted into the cylinder head. This method is constrained by the limited space available in cylinder heads of modern SI engines [7,8]. Additionally, water injection is only needed in high engine load when knock occurs, the DI injector tip is therefore exposed to high thermal load when engine is at light and medium load conditions. It is necessary to inject a minimum amount of water to cool the injector and reduce attrition. This requires sophisticated injection strategies and water-efficient operation. On the contrary, water injection into the intake manifold uses lower injection pressure so that small and inexpensive water pumps and simple control systems can meet the needs. The injected water vaporizes during the intake process, which reduces the air temperature and increases the air density, leading to higher volumetric efficiency. Furthermore, the water can be well mixed with fresh charge and be delivered without condensation. A proportion of the liquid water droplets enter the cylinder and evaporate during the compression stroke, resulting in reduced in-cylinder pressure buildup as well as temperature. Generally, water port injection (WPI) method is the most cost-effective water injection strategy that is widely investigated by the scholars and applied on production vehicles [7,9].

Boretti [10] explored the use of WPI in a single cylinder turbocharged DI SI engine. It was found that with 7% of WPI, the engine maximum air flow rate was raised from 570 kg/h to 670 kg/h, thermal efficiency was increased 2% due to the inhibition of knocking and exhaust temperature was averagely reduced 100 K. Bosch improved BMW M4 GTS engine by adding a WPI system after the intercooler. WPI is applied when the engine is approaching or at full load conditions. The extra cooling brought by water evaporation effectively suppresses knock tendency and constricts the use of mixture enrichment, resulting in increases of 37 kW engine power output, 50N/m torque and 13% fuel efficiency [11,12]. Finally, the M4 3.0T DI SI engine possesses ultra-high specific power of 120 kW/L. Kim et al. experimentally tested the effect of water injection on a 1.6L naturally aspirated prototype engine with compression ratio of 13.5 [12]. The results showed that water injection can substantially mitigate knock occurrence, allowing more advanced spark timing and less use of fuel enrichment. The high compression ratio coupled with the water injection technology enable the engine to have a thermal efficiency of 45%. Lanzafame et al. [13] conducted research on a CFR engine and reported that Research Octane number (RON) increased from 70 to 93 and Motor Octane number (MON) from 64 to 90 by simultaneous increase of compression ratio and water injection. Apart from the great charge cooling effect for knock mitigation, water injection could also reduce pollutant emissions. Experimental data [14] indicated that NO emissions reduced by 50% with water/fuel ratio in the range from 1 to 1.25 at maximum break torque (MBT) spark timing. Wang et al. [15,16] investigated the mechanism of water injection on NO_X reduction. I was found that the enhanced thermal capacity of the fresh charge with water injection reduced the combustion temperature which led to the reduction of NO formation. From the chemical aspect, water vapor could reduce the concentration of O radicals by the scavenging reaction, which were crucial for thermal NO formation [17]. It also reported that with a water/gasoline ratio of 1, more than 80 % of NO_X emission could be cut down. Finally, Hoppe et al. [18] experimentally tested DI water in a 500cc single cylinder SI research engine and found that advancing water injection timing resulted in a trade-off between fuel consumption and NO_X emissions. The maximum NO_X reduction was realized in full load

condition when water was injected at the timing of intake valve closing.

As reviewed above, most researches on water injection technology were not based on the production engines which may decrease the reliability of the experimental outcomes. As a technology aiming for further enhancing the engine specific power output, it is necessary to perform a research on the state of art engines. In this study, experiments were conducted on a 135 kW 1.5L turbocharged DI SI production engine with compression ratio of 11.7 and miller cycle. Tests were performed at full-load characteristic curves to find the potential gain of WPI.

2. Experimental apparatus and procedures

Figure 1 shows the schematic of the test engine. The test system includes an experimental engine, an engine control and acquisition system (items 8, 11 and 18-22), an eddy current dynamometer (items 9 and 10), a fuel supply system (items 15 and 17), a water injection system (items 1-6 and 12), an emission measurement system (item 20), and an in-cylinder combustion analyzer (items 14 and 16). The major components of the engine system are described as follows.
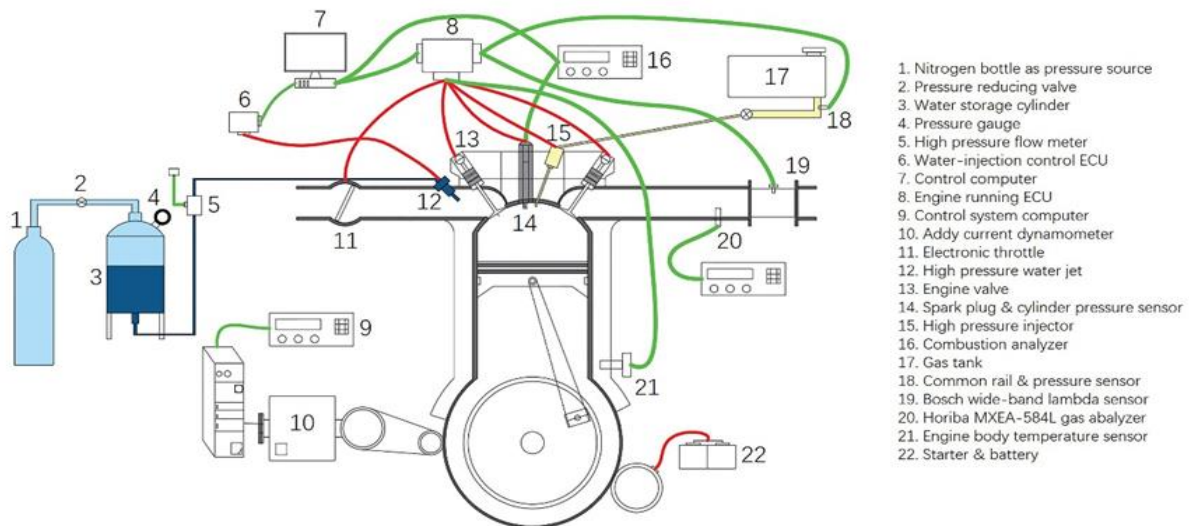

1. Nitrogen bottle as pressure source
2. Pressure reducing valve
3. Water storage cylinder
4. Pressure gauge
5. High pressure flow meter
6. Water-injection control ECU
7. Control computer
8. Engine running ECU
9. Control system computer
10. Addy current dynamometer
11. Electronic throttle
12. High pressure water jet
13. Engine valve
14. Spark plug & cylinder pressure sensor
15. High pressure injector
16. Combustion analyzer
17. Gas tank
18. Common rail & pressure sensor
19. Bosch wide-band lambda sensor
20. Horiba MXEA-584L gas abalyzer
21. Engine body temperature sensor
22. Starter & battery

Figure 1. Schematic of the engine system.

2.1. Engine and Instrumentation

In this study, experiments were conducted on a 135kW 1.5L turbocharged DI SI production engine with compression ratio of 11.7 and miller cycle. Specifications of the test engine are shown in Table 1. As shown in the Figure 1, the dynamometer used in the experiments is a model CW160 eddy current dynamometer produced by Kaimai (Luoyang) Electromechanical Co., Ltd. and the engine bench numerical control device is model FST2D. The fuel supply system is composed of a high-pressure fuel pump, a fuel rail and an injector. The DI fuel pressure of the original engine is 15 MPa. The in-cylinder pressure was measured by a Kistler 6115B on the spark plug and sampling frequency was 200 times at per cycle. An AVL Model 642 combustion analyzer was used for the analysis of the combustion characteristics and the determination of the engine operating limit. Smoke emissions were monitored by an AVL 415 filter-type smoke meter as filter smoke number (FSN). The filter paper smoke is 1 FSN = 1 PS when the effective length of the column is 405 mm at 25 ° C, 1 bar. Each experimental condition was repeated at least three times to determine the measurement uncertainties using the method given in Ref. [19]. The uncertainties of the testing devices are shown in Table 2.

4

Table 1. Specifications of test engine.

Engine type	L4, four-stroke, water cooling
Compression ratio	11.5
Bore x stroke	75mm x 84.8mm
Engine capacity	1.5L
Intake and exhaust control	VVT
VVT adjustment range	0-60 CAD
Intake Valve Open	352.5 CAD
Intake Valve Close	582.5 CAD
Exhaust Valve Open	149 CAD
Exhaust Valve Close	336 CAD
Fuel supply	Direct injection
Water supply	Port injection

Table 2. Measurement uncertainties.

Device	Associated measurement uncertainty
Engine speed	0.25% of full scale
Torque	0.03 of the output voltage
Air volumetric flow rate	4.0% of the measurement
Gasoline mass flow rate	1.8% of the measurement
Water mass flow rate	1.9% of the measurement
In-cylinder pressure	0.45% of full scale
HC concentration	3.1% of the measurement
NO concentration	3.5% of the measurement
CO concentration	3.1% of the measurement
Filter smoke number	2.8% of the measurement
Bosch lambda sensor	1.6% of the measurement

2.2. Water injection system

The surface tension of water (72 mN/m) is much larger than that of gasoline (22 mN/m). To provide a fine water atomization process, a high pressure injection system, which was the same as the GDI system, was used for WPI [20]. The WPI injector was placed about 10 cm upstream from the intake valve, which was the place for the injector of the PFI version of the test engine. The WPI injector was pointing to the back of intake valve. The water was pressurized to 50 bar by nitrogen in a 35 L water tank. The WPI injectors were activated by an independent ECU which was connected with engine onboard ECU through CAN bus to synchronize the crankshaft and camshaft signals. The engine onboard ECU and water injection ECU were controlled through two separate "INCA" software. The injector was statically calibrated to ensure accurate control of the water injection [5]. Figure 2 shows the calibration results of injection flow rates versus injection durations under different injection pressures.
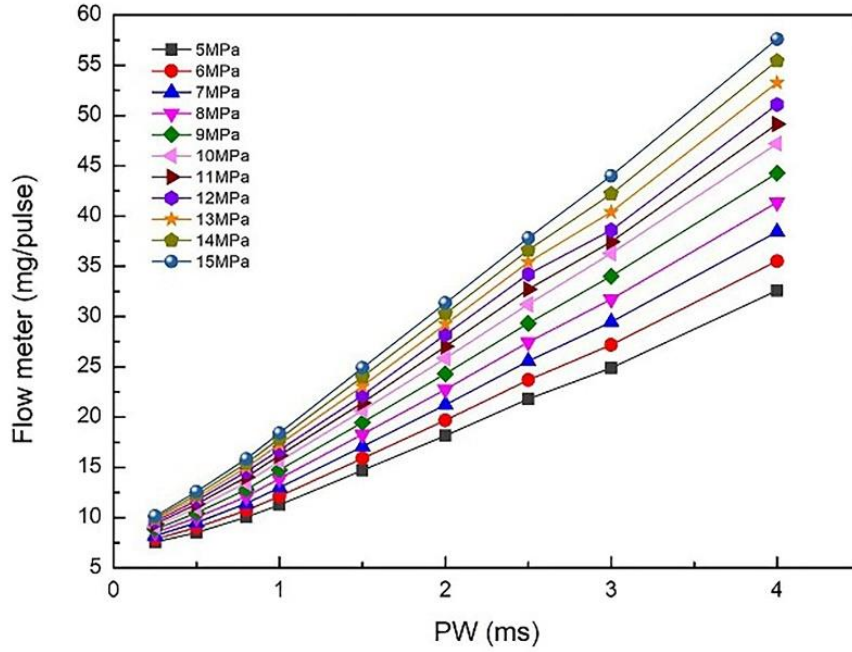
Figure 2. Calibration of water injection flow rate of the high-pressure injector under different pulse width (PW) and injection pressure conditions.

2.3. Experimental procedure

The engine was first warmed up and the throttle valve was gradually opened to wide open throttle (WOT) after the circulating water temperature was around 90 ± 3 °C [21,22]. As the engine was running according to its original MAP which normally run the engine at knock limited spark advance (KLSA) under WOT condition. Sporadic knock could be monitored from both audible source and AVL INDICOM combustion analyzer, which was regarded as original KLSA. The water was then injected into the intake port and the water/gasoline ratio was gradually raised to explore the effect of water injection on knock mitigation and engine performance at original KLSA. Later, at each tested water/gasoline ratios, the spark timing was advanced until knock was detected. The spark timing was then retarded 1 CAD and marked as adjusted KLSA. It should be noted that the engine knock was detected through monitoring the cylinder pressure trace. It was regarded as knock condition if 10 out of 100 consecutive cycles were detected with noticeable pressure wave oscillations (peak to peak oscillation over 1 bar).

All the tests were conducted at 1500 rpm and WOT condition where the propensity of knock was larger than other conditions. As the tested engine condition was far from maximum load condition (full load and full speed) where the fuel enrichment was needed to protect the engine component, the air/fuel ratio was kept at stoichiometric value dominated by the on broad ECU. Two injection timings 360 and 170 °CAD BTDC [23,24], which represented water injection before and after the intake valve closed (IVC), respectively, were selected as the baseline injection timings to explore the effect of water injection timing on knock mitigation and engine performance [5,25]. It should be noted that in the experiment, the ratio of gasoline to water is the volume ratio.

COV_{IMEP} is calculated using equation (1) where IMEP is the indicated mean effective pressure of each engine cycle.

$$COV_{IMEP} = \sqrt{\sum_{i=1}^{k}(IMEP_i - \overline{IMEP})^2/(k-1)}/\overline{IMEP} \qquad (1)$$

3. Results and Discussion

Figure 3 shows the effects of water injection ratio and injection timing on knock limit spark angle (KLSA). Overall, the KLSA at an engine full-load characteristic operating point is determined on the basis of the engine MAP and knock sensor. As shown in Figure 3, without WPI (lines marked with before adjust), the original KLSA is maintained between 2.5-2.0 °CAD ATDC. When WPI starts, the injected water reduces the chemical react activity, shifts the chemical equilibrium to the side of reactants and dilutes the in-cylinder mixture, which elongates the ignition delay, prolongs the combustion duration and most importantly, quenches the pre-ignition of end gas. As a result, the spark advance (SA) can be forwarded [26,27]. As shown in Figure 3, as the water/gasoline volume percentage increases from 0% to 50%, the adjusted KLSA (lines marked with after adjust) can advance from -2.5 to 3 °CAD BTDC at both 170 and 360 °CAD BTDC WPI timings. It also can be seen that there is a deviation of KLSA at WPI timing of 170 °CAD and 360 °CAD when the water/gasoline volume ratio is in the middle level range between 15% and 40%. This may be attributed to the difference in the WPI timing. When the water/gasoline volume ratio is at low level (less than 15% in this test), the small quantity of water may easily evaporate regardless the WPI timing. When the water/gasoline volume ratio is greater than 40%, the large amount of water may encounter evaporation problem, meaning the water cannot fully evaporate and water film on the in-take port may form, no matter the change of WPI timing. The actual amount water vapor into the cylinder may reach the same level when the water/gasoline volume ratio is higher than 40% , so the effect of WPI on KSLA at WPI timing of 170 °CAD and 360 °CAD is similar. It should be noted that the adjusted KLSA is determined by the AVL INDICOM combustion analyzer in which a cylinder pressure oscillation less than 1.0 bar is set as the borderline of determining KLSA. Over this range the knocking may jeopardize the engine [28].
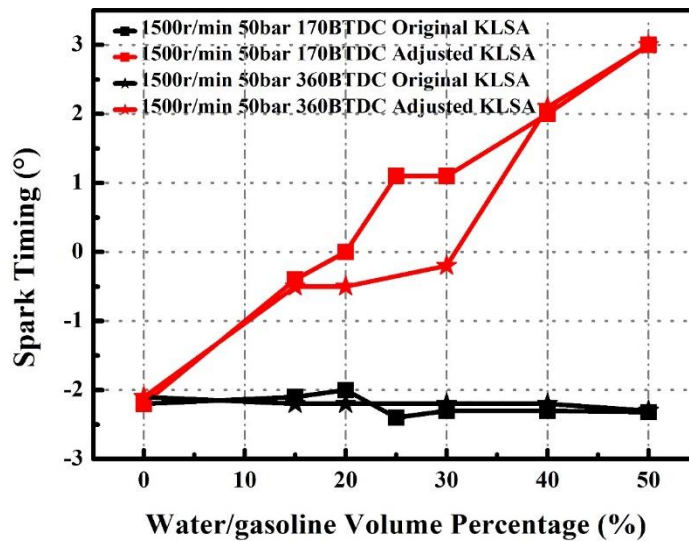

Figure 3. Effect of water injection ratio and injection timing on KLSA.

Figure 4 illustrates the effect of water injection ratio on indicated mean effective pressure (IMEP) at two WPI timings of 170 and 360 °CAD BTDC. As shown in the Figure 4, at original KLSA, with the raise of water/gasoline ratio, IMEP is gradually lowered from 19.2 to 18.1and 17.9 bar at WPI timing of 170 and 360 °CAD BTDC, respectively. Whereas at the adjusted KLSA condition, IMEP increases from 19.2 to 20.4 at WPI timing of 170 °CAD BTDC and 20.3 bar at WPI timing of 360 °CAD BTDC. When water/gasoline percentage is below 15%, IMEP increases by approximately 5% (or 0.9 bar). The increase trend of IMEP slows down when water/gasoline percentage is above 15%. The peak IMEP reaches 20.5

bar at water/gasoline percentage of 30% and then IMEP starts to decline with further increase of water/gasoline percentage. Nevertheless, the IMEP still remains above 20 bar at higher water/gasoline percentage. At original spark timing, WPI negatively affects the flame kernel formation process and slows down the combustion process, resulting in retarded combustion phase and longer combustion duration. Thus, IMEP reduces with the increase of water/gasoline percentage. At adjusted KLSA, the advanced spark timing compensates the combustion phase delay caused by WPI and IMEP increases with the raise of water/gasoline percentage within 30%. Excess water injection (>30%) decreases IMEP. This would be because water cannot evaporate completely due to its low evaporation speed and high latent heat, so that some liquid water mist may still exist in the cylinder before combustion which has a destructive effect on the flame propagation process [7]. The decline of IMEP when the water/gasoline percentage exceeds a certain level was also reported in Refs. [29,30].
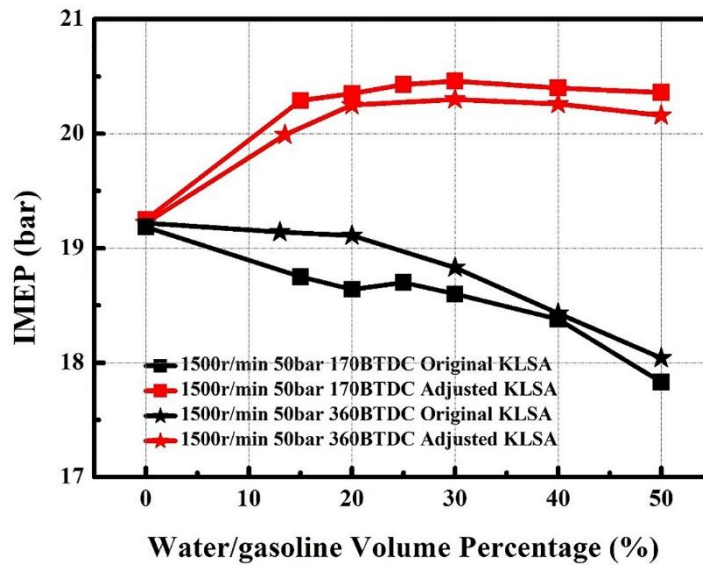

Figure 4. Effect of water injection ratio and injection timing on IMEP.

Figure 4 also shows that, at original spark timing, IMEP at WPI timing of 360 °CAD BTDC is higher than that at WPI timing of 170 °CAD BTDC. This is because the intake valve open timing is between 352.5-582.5 °CAD (Table 1) and WPI timing of 360 °CAD BTDC is during this period. Thus, part of the water spray is likely to directly enter the combustion chamber, which reduces the in-cylinder temperature and increases the volumetric efficiency. On the other hand, intake valve is closed for WPI timing of 170 °CAD BTDC and its effect on improving volumetric efficiency is limited (Figure 5). Consequently, IMEP at WPI timing of 360 °CAD BTDC is greater than that at WPI timing of 170 °CAD BTDC. Under the adjusted KLSA condition, IMEP of 170 °CAD BTDC WPI timing is greater than that of 360 °CAD BTDC WPI timing. The IMEP results in Figure 4 clearly show that excessive water/gasoline percentage (>30% in this study) has adverse impacts on the combustion performance and adjusting the ignition advance angle cannot compensate these adverse impacts (i.e. IMEP reduction). Therefore, higher water/gasoline percentages are not investigated. Similar results were also reported [29,31].

Figure 5 demonstrates the effect of water/gasoline volume ratio on volumetric efficiency at WPI timings of 170 and 360 °CAD BTDC. The volumetric efficiency η_v is calculated based on equation (2) as the ratio between the actual (measured) volume of intake air V_a [m^3] drawn into the cylinder of the engine and the theoretical volume of the engine cylinder V_d [m^3], during the intake engine cycle. Error bars represent the uncertainty range and are calculated through 500 consecutive measurements by the inlet air flow meter via INCA system with a sampling rate of 25 Hz. As shown in Figure 5, volumetric efficiency is 97.2% without WPI. When WPI is applied, volumetric efficiency generally increases with the raise of

water/gasoline ratio except for WPI timing of 360 °CAD BTDC with adjusted KLSA. Volumetric efficiency at WPI timing of 170 °CAD BTDC is generally lower than that at 360 °CAD BTDC. This is because WPI timing of 360 °CAD BTDC is during the intake valve open, so that part of the water spray enters the combustion chamber directly and cools the intake air and increases the air density, leading to higher volumetric efficiency. WPI timing of 170 °CAD BTDC does not have such cooling effect as the whole water injection process is taken place when the intake valve is closed.

$$\eta_v = V_a/V_d \qquad\qquad (2)$$
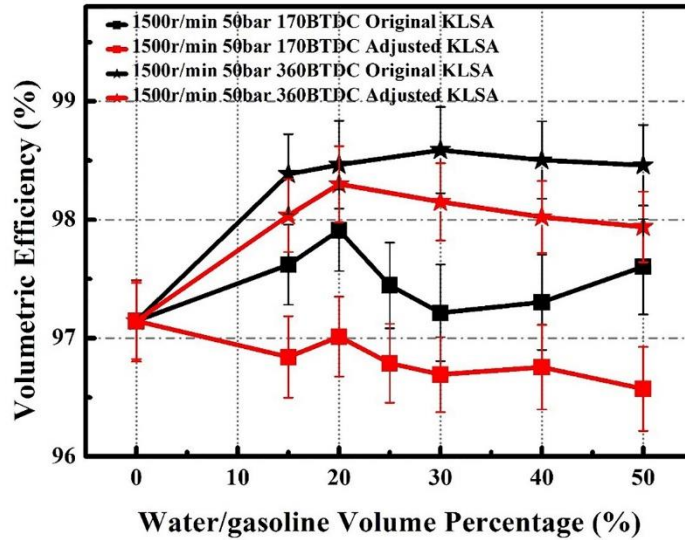
Figure 5. Effect of water injection ratio and timing on volumetric efficiency.
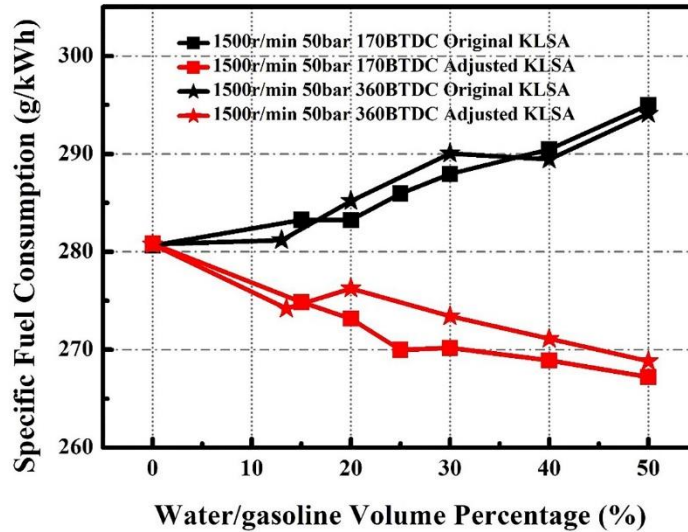
Figure 6. Effect of water injection ratio and timing on fuel consumption.

Figure 6 shows the specific fuel consumption rate as a function of water/gasoline percentage at WPI timings of 170 and 360 °CAD BTDC. Evidently, at original KLSA, fuel consumption gradually increases from 280g to 295 g/kWh with the increase of water/gasoline percentage. However, at adjusted KLSA, fuel consumption gradually declines from 280 to 268 g/kWh. Figure 6 also shows the impact of the water injection timing on fuel consumption is insignificant. Therefore, through proper adjustment of water/gasoline percentage and spark timing, WPI technology is capable of reducing the specific fuel consumption.

Figure 7 demonstrates the correlations between the exhaust and intake temperatures and the water/gasoline percentage. As shown in Figure 7(a), at original KLSA, the exhaust gas temperature is between 730 and 740 °C. It slightly increases with the raise of water/gasoline percentage within 30%, and then reduces back to 735 °C with further increase of water/gasoline percentage to 50%. At adjusted KLSA, the exhaust temperature drops rapidly from 730 to 675 °C with the increase of water/gasoline percentage. Meanwhile, WPI timing has little impact on exhaust temperature.
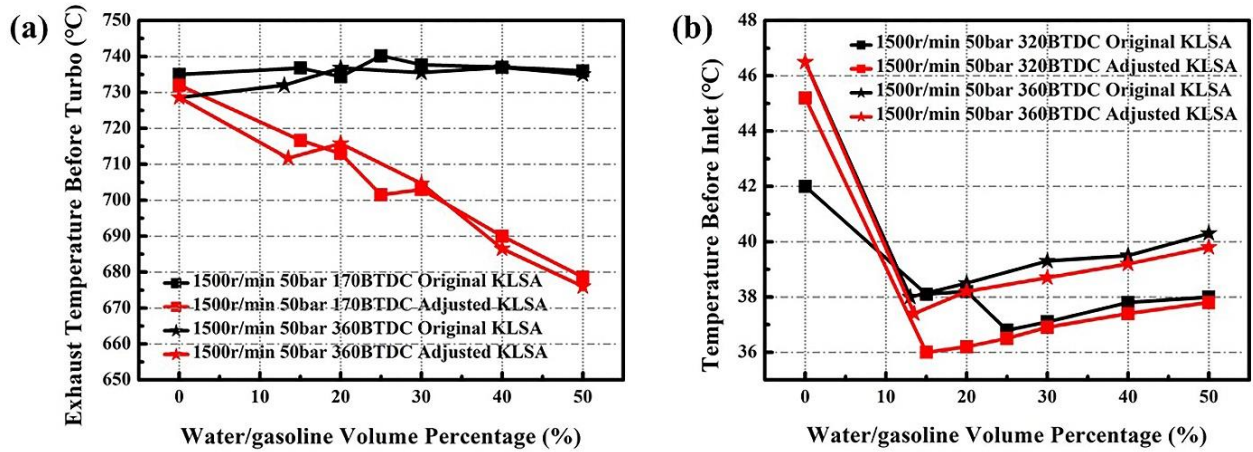
Figure 7. Effect of water injection ratio and timing on exhaust (a) and intake (b) gas temperatures.

At original KLSA condition with water/gasoline percentage below 30%, the increase of exhaust gas temperature is caused by the delay of combustion phase and prolong of combustion duration (Figure 10). This leads to significant post-combustion, and consequently higher exhaust gas temperature. When water/gasoline percentage is over 30%, the strong cooling effect of WPI significantly reduces the combustion temperature, as well as the exhaust temperature. At the adjusted KLSA condition, the combustion phase is advanced and combustion duration is shortened, leading to less after-burning and thus lower exhaust temperature.

The effect of WPI on intake air temperature is shown in Figure 7(b). The intake temperature is measured by a temperature sensor installed in the intake port at about 10 cm downstream the WPI injectors and 4.5 cm upstream the intake valve (Figure 1). Figure 7(b) shows that the intake air temperature is kept between 42 and 46.5 °C without WPI. When WPI is applied (<15%), the intake temperature reduces obviously to 36-38 °C. When water/gasoline percentage is greater than 15%, the intake temperature raises slowly again and reaches 38-40 °C when water/gasoline percentage is 50%. This is because a Bosch GDI injector was used for the water injection without any modification in this study, which lead to poor water atomization and in-take port wall welling. When water/gasoline percentage is greater than 15%, water impingement on intake port becomes severe and the evaporation of such water does not absorb heat from air but from intake port and valve seat.

Figure 8 shows the effect of water/gasoline percentage on COV_{IMEP} with different water injection timings. COV_{IMEP} is primarily a reflection of the stability of combustion. As shown in Figure 8, COV_{IMEP} is stable between 1.5% and 1.6% without WPI. At original KLSA condition, COV_{IMEP} increases quickly with the increase of water/gasoline percentage. COV_{IMEP} reaches 2.25% under water/gasoline percentage of 50%. At adjusted KLSA condition, COV_{IMEP} is maintained between 1.4% and 1.6% when water/gasoline percentage increases from 0% to 50%. Generally, without the advancement of spark timing, WPI leads to unstable combustion (higher COV_{IMEP}).

Figure 9(a) illustrates the effect of the water/gasoline percentage on in-cylinder pressure at injection timings of 170 and 360 CAD BTDC. At original KLSA condition, in-cylinder pressure without WPI is

larger than that with WPI. This is because WPI leads to incomplete fuel combustion. Figure 9(a) also shows that WPI lowers the peak in-cylinder pressure and delays its phase. The phase delay increases with the increase of water/gasoline percentage. This is due to the temperature drop and dilution effect caused by WPI. The evaporation of water droplets cools the mixture temperature before combustion. Further, the vaporized water occupies some cylinder volume so that the density of the oxygen is diluted. These two factors slow down the combustion rate, lead to elongated combustion duration, retard combustion phases and finally decrease peak pressure (P_{max}).
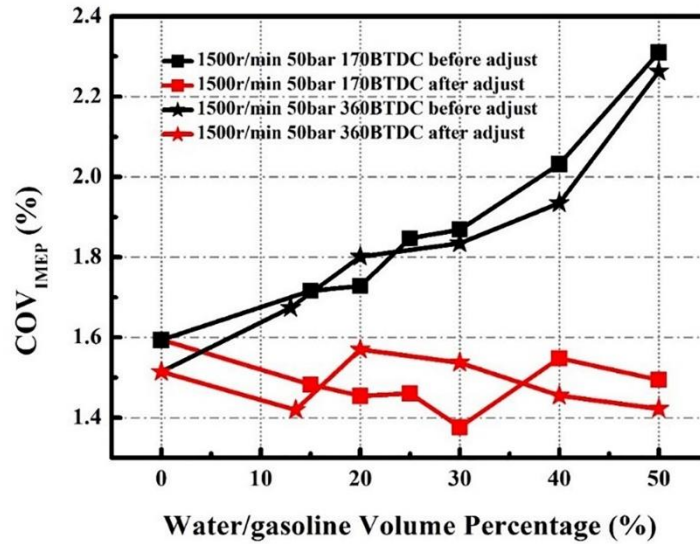

Figure 8. Effect of water injection ratio and timing on COV_{IMEP}.
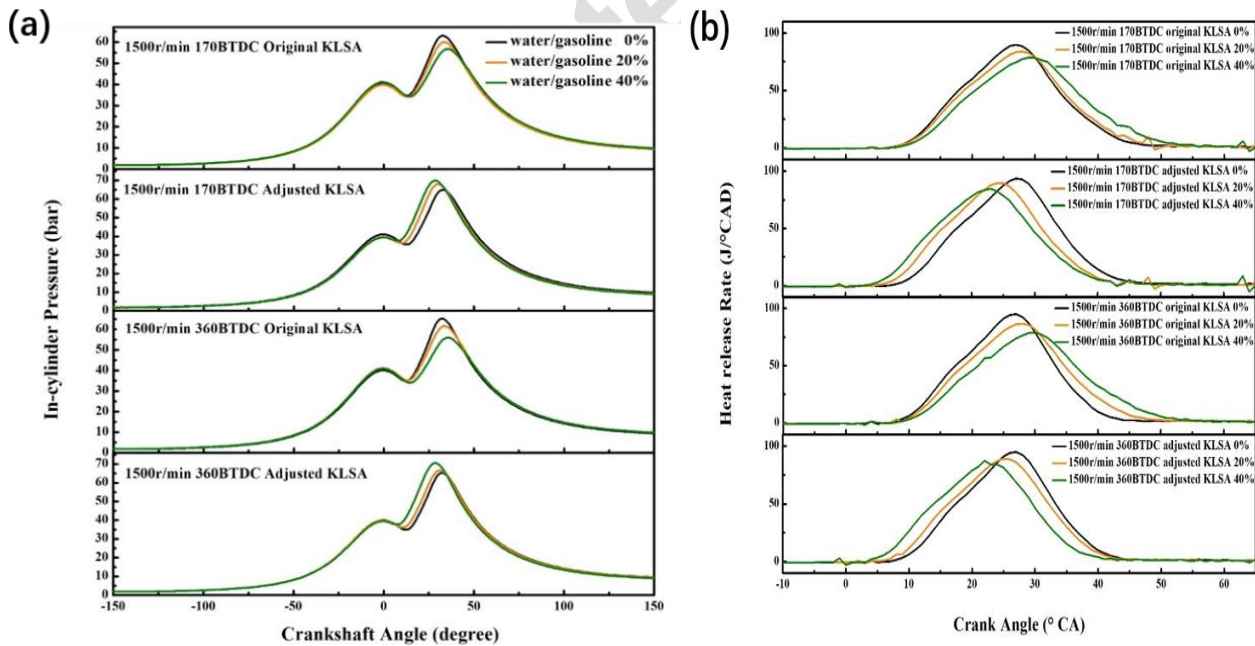

Figure 9. Effect of water injection ratio and timing on in-cylinder pressure (a) and heat release rate (b).

At adjusted KLSA condition, the peak in-cylinder pressure increases and its phase advances with the raise of water/gasoline percentage. This is because the spark advance increases with the raise of water/gasoline percentage. Higher spark advance leads to earlier combustion (at smaller cylinder volume) and consequently higher peak in-cylinder pressure and earlier combustion phase. Detailed analysis of combustion process is elaborated in Figure 10.

The heat release rates of different water/gasoline volumetric ratios at two injection timings of 170

and 360 CAD BTDC are compared in Figure 9 (b). At original KLSA condition, the peak of the heat release curve decreases with the raise of water/gasoline percentage and the position of the peak are retarded as well. Also, the heat release curves at WPI conditions are wider than the corresponding gasoline only condition. Apparently, at original KLSA condition, the addition of water delays the combustion phase and prolongs the combustion duration. At adjusted KLSA condition, the advance of spark timing makes the position of the heat release peak earlier than the gasoline only condition. However, the peak values of heat release curves at WPI condition are still lower than the gasoline only condition. Comparing with the corresponding cylinder pressure curves at Figure 9 (a), it can be seen that the peak cylinder pressures of WPI at adjusted KLSA condition are actually higher than the gasoline only condition. This indicated that the higher in-cylinder pressure at adjusted KLSA condition are mainly due to the advance of combustion phase which makes the combustion happens in smaller cylinder volume. Generally, the combustion process (heat release rate) is negatively affected by the WPI and cannot be compensated by solely advance of spark timing.

Figure 10 demonstrates the effect of water/gasoline percentage on combustion phases. The combustion phases include CA50, CA0-5, CA0-10, CA10-50 and CA10-90. CA50 refers to crank angle position where 50% accumulated heat is released. CA0-5 refers to the flame kernel formation process and it is defined as the period from spark discharge to formation of steady flame kernel. The combustion initiation duration (CA0-10) is defined as the crank angle degrees from spark timing to when 10% of fuel mass burnt. Normally, shorter CA0-10 means better combustion stability and quality. The early combustion duration (CA10-50) is defined as the crank angle degrees from 10% to 50% of fuel mass burnt. It is often used to evaluate the combustion efficiency. The major combustion duration (CA10-90) is defined as the crank angle degrees from 10% to 90% of fuel mass burnt. It directly affects the engine thermal efficiency. Longer the combustion duration means more heat loss through the cylinder wall.

As shown in Figure 10(a), CA50 stays around 27 °CAD ATDC without WPI. When WPI is applied, CA50 slightly increases to 31 °CAD ATDC with the increase of water/gasoline percentage from 0% to 50%. Evidently, WPI has a distinct impact on delaying combustion phase. It is generally regarded that keeping CA50 between 8 and 10 °CAD ATDC can have the optimum engine efficiency. In this study, as the engine is working at its full-load condition, CA50 is delayed purposely to avoid severe knock and protect the engine. At adjusted KLSA condition, spark advance increases with the increase of water/gasoline percentage. The reduced in-cylinder temperature, diluted charge and decreased laminar flame temperature and elongated ignition delay caused by water addition gives more space for spark timing advancement[36][37]. Consequently CA50 advances from 27 to 22 °CAD ATDC. This leads to the decrease of specific fuel consumption (Figure 6) and increase of thermal efficiency (Figure 12).

In an engine equipped with WPI system, adjustment of spark timing can effectively counteract the negative impact of WPI on combustion and further increase the thermal efficiency. As shown in Figures 10(c) and 10(d), at original KLSA, CA0-5 gradually increases from 13.5 to 16 °CAD and CA0-10 gradually increases from 15.5 to 18 °CAD with the increase of water/gasoline percentage. After the optimization of the spark advance, CA0-5 and CA0-10 are maintained at approximately 13.5 and 15.5 °CAD, respectively. Apparently, WPI has a negative impact on formation of flame kernel and preliminary flame development. These results may because the water (H_2O) has a great third body efficiency which is about 10 times higher than that of nitrogen (N_2). Therefore, the addition of H_2O accelerates the third body reaction rate and radicals of O, OH and H are all reduce, leading to a low thermal reaction speed. These findings also agree with the previous studies that the existence of steam may hamper the low temperature chemical reaction in the flame kernel formation process, and dilution effect and reduced temperature caused by water evaporation can reduce the laminar flame speed [**Error!**

Nevertheless, through the optimization of spark advance, the negative impact of WPI on CA0-5 and CA0-10 can be offset.
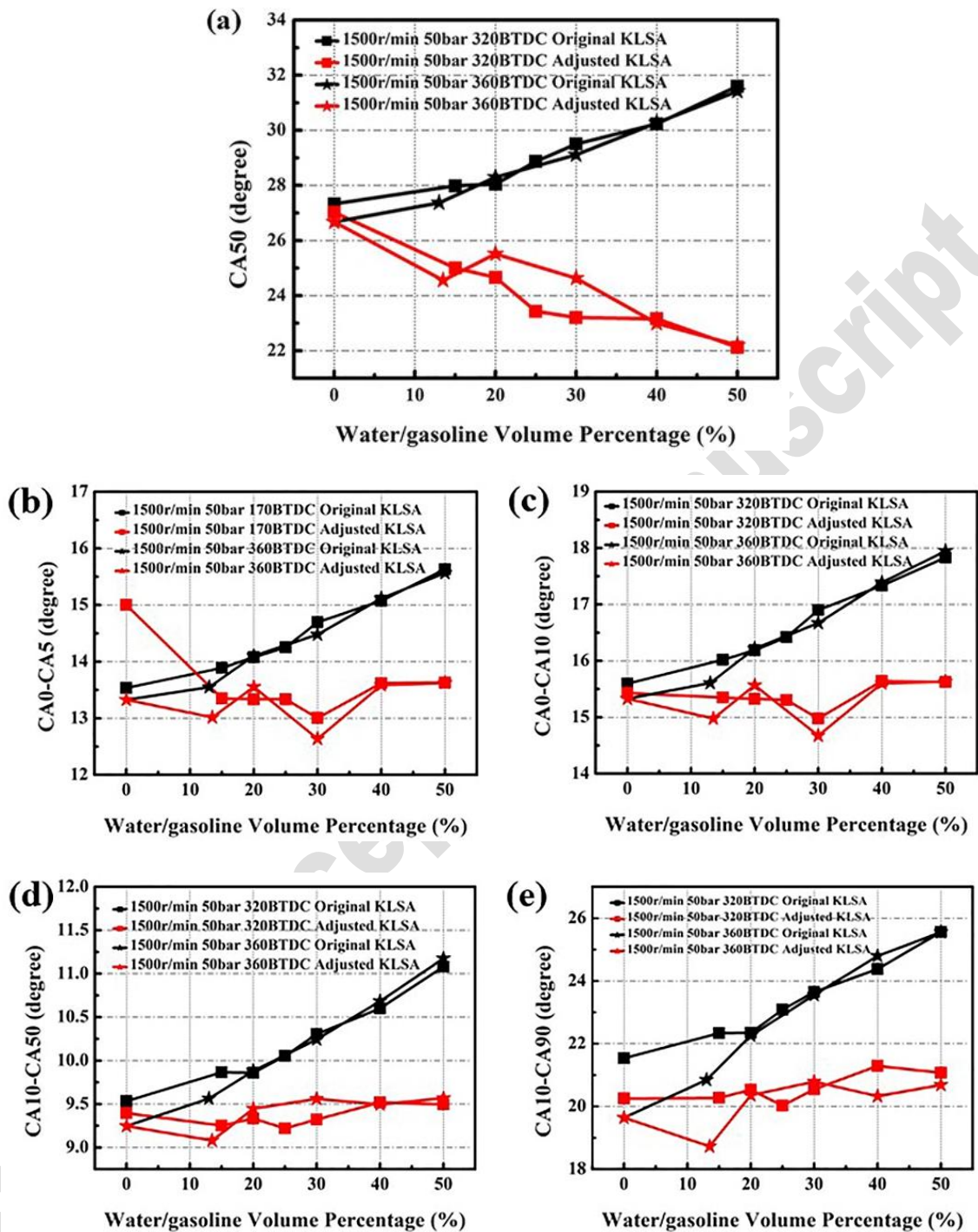

Figure 10. Effect of water injection ratio and timing on combustion phases.

Figure 10(e) also shows that, at original KLSA, CA10-50 and CA10-90 increase from 9.5 and 16.5 °CAD to 11.25 and 18.0 °CAD, respectively, with the increase of water/gasoline percentage. After the adjustment of spark timing, CA10-50 is stable at 9.5 °CAD and CA10-90 stays around 15.75 °CAD. Again, it shows clearly that the existence of steam (from WPI) in the mixture reduces the flame propagation speed, and higher initial temperature and pressure (by more speak advance) can offset such negative impact.

Generally, WPI has negative impacts on flame kernel formation, combustion initiation duration, early

combustion duration and major combustion duration. However, these impacts also reduce the likelihood of pre-ignition, which is especially important at full load condition when destructive super-knock may occur. The advancement of spark timing can eliminate these negative impacts on combustion processes. More importantly, it allows more spark advance to achieve higher IMEP without knock. Nonetheless, as the WPI steam lowers the volume fraction of oxygen in the intake fresh charge, flame propagation speed at adjusted KLSA condition are still lower than the without WPI condition (Figures 10(d) and 10(e)). Similar results were also reported in Ref. [26].

To further analysis the effect of WPI on combustion process, peak pressure rise rate (R_{max}) and peak in-cylinder pressure (P_{max}) are illustrated in Figures 11. These parameters are also indexes indicating the occurrence of knock and the intensity of combustion [26]. As shown in Figure 11 (a), R_{max} is maintained at around 2.6 bar/°CA without WPI. At original KLSA condition, R_{max} declines by 40% from 2.6 to 1.6 bar/°CA when water/gasoline percentage increases from 0% to 50%. At adjusted KLSA condition, R_{max} fluctuates around 2.8 bar/°CA regardless the increase in water/gasoline percentage. This indicates that WPI leads to deterioration of combustion and thus lower pressure rise rate when spark advance is un-optimized. With the advance of spark timing, WPI enables the engine to work under higher R_{max} without knock issue. Similarly, Figure 11(b) shows that Pmax of original KLSA condition decreases from 68 to 55 bar but Pmax of adjusted KLSA condition increases from 68 to 75 bar when water/gasoline percentage increases from 0% to 50%. Therefore, WPI can effectively lower the tendency of knock.
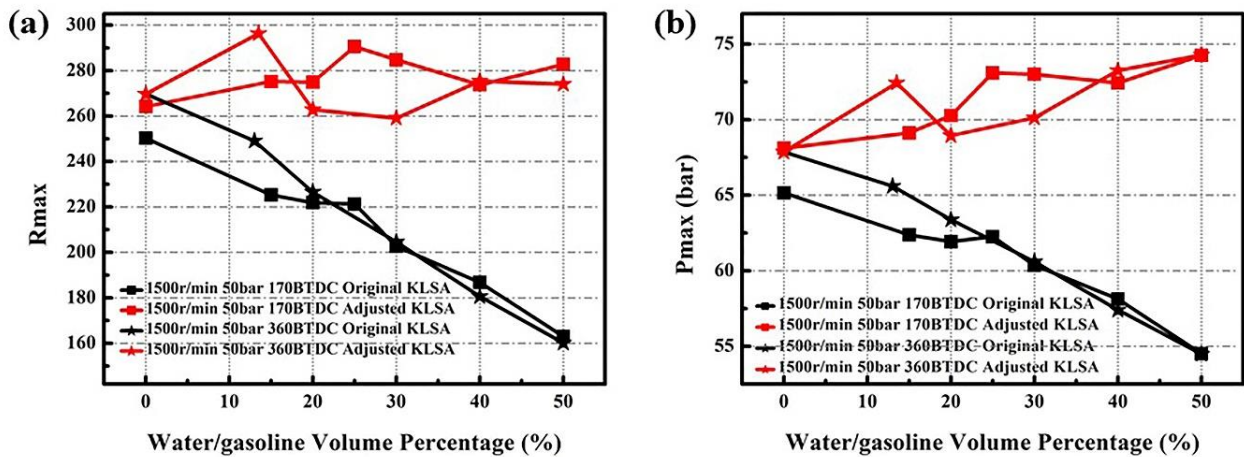

Figure 11. Effect of water injection ratio and timing on R_{max} and P_{max}.

The effect of water/gasoline percentage on thermal efficiency is shown Figure 12. The engine thermal efficiency is 29.25% without WPI. At original KLSA, the thermal efficiency gradually declines to 27.75% with the increase of the water/gasoline percentage, and WPI timing does not show significant impact on thermal efficiency. At adjusted KLSA condition, thermal efficiency increases from 29.25% to 30.5% when WPI is applied and the thermal efficiency at WPI timing of 170 °CAD BTDC is greater than that at 360°CAD BTDC. The above analysis on Figures 10 and 11 have demonstrated that WPI at original KLSA hampers the flame kernel formation (CA0-5) and elongates combustion durations. These lead to the decrease of thermal efficiency with increase of water/gasoline percentage. At adjusted KLSA, all the combustion indexes shown in Figures 10 and 11 are rehabilitated through the advance of spark timing. Moreover, R_{max} and P_{max} reach even higher values as compared with that at none-WPI condition. Thus, thermal efficiency of adjusted KLSA is greater than that at original KLSA. This demonstrates the potential of WPI technology on further improving engine thermal efficiency. Figure 12 also shows that, at adjusted KLSA condition, thermal efficiency increases more at WPI timing of 170 °CAD BTDC than that at 360 °CAD BTDC. This would be because intake valve is closed at 170 °CAD BTDC. This allows more

time for water and air to mix in the intake manifold and reduces water droplets or mist entering into the combustion chamber. The water droplets or mist have a strong hindrance on the combustion and flame propagation [31].
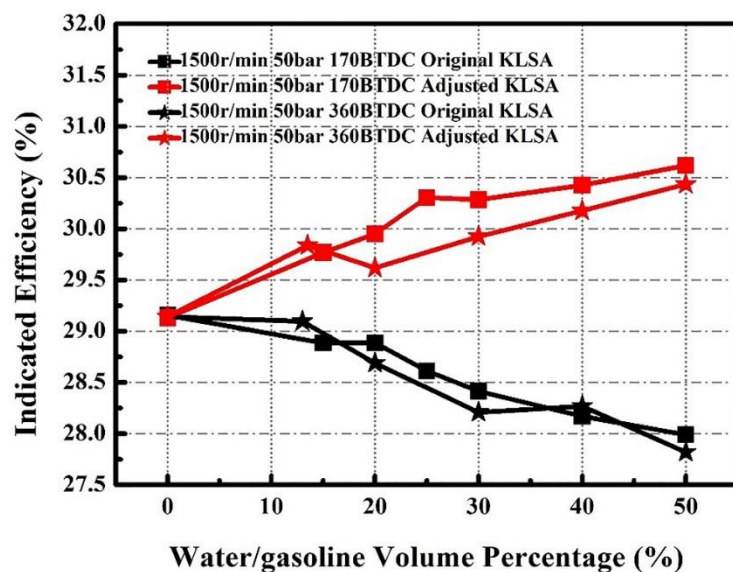

Figure 12. Effect of water injection ratio and timing on Indicated thermal efficiency.
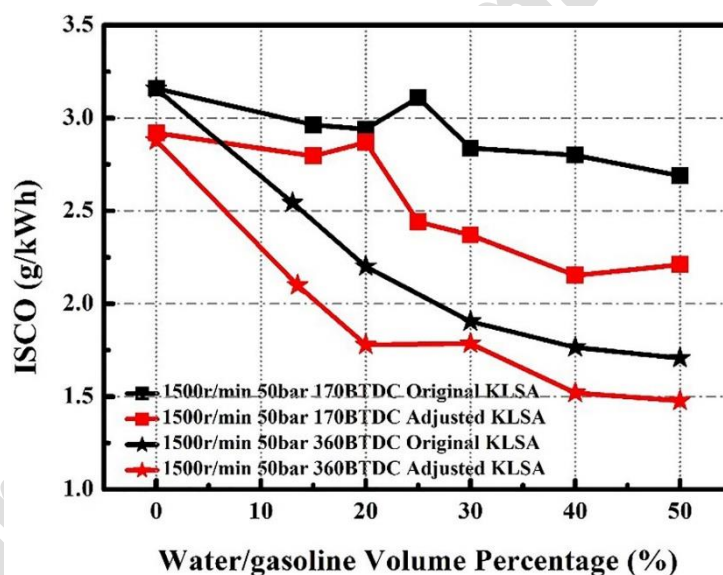

Figure 13. Effect of water injection ratio and timing on ISCO.

The variations of indicated specific carbon monoxide (ISCO) and hydrocarbon (ISHC) emissions with water/gasoline percentage are shown in Figures 13 and 14. As shown in Figure 13, ISCO continuously decreases at all tested conditions with the increase of water/gasoline percentage. At original KLSA condition, ISCO decreases from 3.2 to 2.7 g/kWh at WPI timing of 170 °CAD BTDC and to 1.75 g/kWh at WPI timing of 360 °CA BTDC. At adjusted KLSA condition, ISCO reduces from 2.9 to 2.2 (170 °CAD BTDC) and 1.5 (360 °CAD BTDC) g/kWh. The kinetic models propose three reactions that lead to in-cylinder CO consumption [32]: $OH + H_2 \leftrightarrow H + H_2O$, $OH + OH \leftrightarrow O + H_2O$, and $CO + OH \leftrightarrow CO_2 + H$. Water injection is expected to increase the OH concentration in the cylinder, which is conducive to the oxidation of CO. This study agrees well with previous studies on CO emission [21,27].

Figure 14 shows that, at original KLSA condition with WPI timing of 170 °CAD BTDC, ISHC first reduces from 12 to 9.2 g/kWh when water/gasoline percentage is below 20% and then gradually rises to

11 g/kWh. At original KLSA condition with WPI timing of 360 °CAD BTDC, ISHC increases quickly from 13.5 to 20g/kWh when water/gasoline percentage is within 20% and the increase trend slows down for higher water/gasoline percentages. The variation of ISHC at adjusted KLSA condition shows similar trend with that at original KLSA condition. As shown in Figure 14, at adjusted KLSA condition with WPI timing of 170 °CAD BTDC, ISHC reduces from 14.5 to 12 g/kWh first and then gradually rises to 14 g/kWh. When WPI timing is 360 °CAD BTDC, ISHC first rises quickly from 16.5 to 20.5 g/kWh and when water/gasoline percentage is within 20% and then the increase trend slows down. The results in Figure 14, indicate that WPI timing has significant effect on ISHC. The reason is that the inlet valve is open for WPI timing of 360 °CAD BTDC and the water spray can directly enter the combustion chamber, causing flame quenching and higher HC emissions as a results of incomplete combustion [27]. Furthermore, the evaporation of water substantially reduces the in cylinder temperature, which also increases incomplete combustion. Figure 14 also indicates that ISHC at adjusted KLSA condition is generally higher than that at original KLSA condition. This is can be attributed to the higher Pmax (Figure 11) which traps more HC emissions in crevice volume during the combustion [34][35]. The advanced spark timing reduces the time for in-cylinder water spray to evaporate and the decreased post-combustion (Figure 7) could also cause the lower ISHC at adjusted KLSA condition.
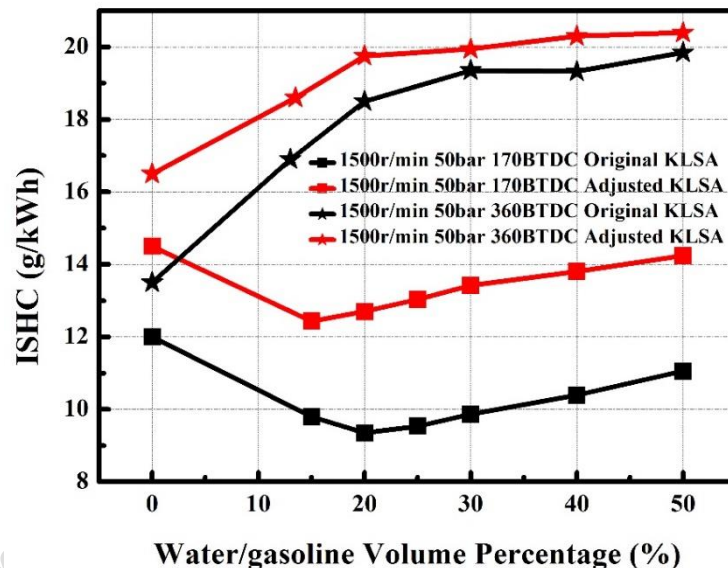

Figure 14. Effect of water injection ratio and timing on ISHC.

Figure 15 demonstrates the variation of indicated specific nitric oxide (ISNO) with water/gasoline percentage. At original KLSA condition, ISNO decreases from 12.5 to 3.46 g/kWh for WPI timing of 170 °CAD BTDC and to 6.12 g/kWh for WPI timing of 360 °CAD BTDC when water/gasoline percentage increases from 0% to 50%. At adjusted KLSA condition, ISNO decreases from 15 to 13.86 and 11.52 g/kWh for WPI timings of 360 and 170 °CAD BTDC, respectively. WPI effectively reduces ISNO emissions and there are four key reasons for this. Firstly, the vaporization of water spray reduces the in-cylinder temperature. Secondly, the steam reduces the oxygen concentration. Thirdly, the heat capacity of the fresh charge is increased by WPI, which reduces the temperature before combustion. Finally, the flame temperature is lowered due to the dilution of water [27]. The formation of NO is related to the in-cylinder temperature, which normally increases with the raise of engine load [15,33]. In this experiment, the engine load is kept constant at the external characteristic condition. ISNO decreases steadily with the increase of water/gasoline percentage, implying that WPI has the potential to substantially reduce NO emissions.
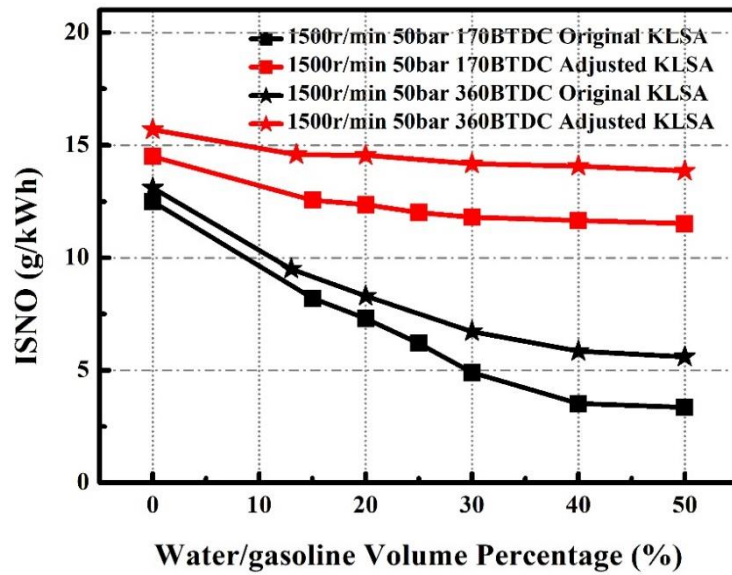
Figure 15. Effect of water injection ratio and timing on ISNO.

Figure 16 illustrates the effect of water/gasoline percentage on exhaust smoke FSN. At original KLSA condition with WPI timing of 170 °CAD BTDC, FSN first declines from 0.05 to 0.045 and then increases to 0.07 with the increase of water/gasoline percentage. At adjusted KLSA condition with WPI timing of 170 °CAD BTDC, FSN fluctuates around 0.04. For WPI timing of 360 °CAD BTDC, FSN gradually declines from 0.035 to 0.018 when water/gasoline percentage is within 30% and then gradually rises to 0.025 at original KLSA and 0.045 at adjusted KLSA. There are two key factors for the formation of soot with WPI [32]. Firstly, the addition of water increases OH radicals which are favorable for the oxidation of soot. Secondly, the concentration of H radicals decreases when steam exists in the mixture, which consequently inhibits the formation of soot kernel as well as the surface growth rate. In addition, the addition of water lowers the combustion temperature which also inhibits the formation of soot. However, FSN increases when water/gasoline percentage is greater than 30%. This would be caused by the deterioration of combustion at high water/gasoline percentage.
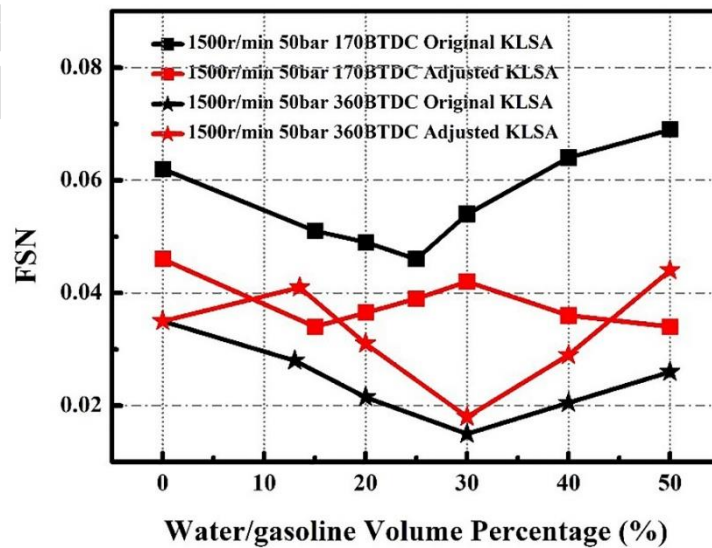

Figure 16. Effect of water injection ratio and timing on FSN.

4. Conclusions

Experiments were carried out on a production 1.5-liter turbocharged GDI engine equipped with a WPI system at 1500 rpm full-load condition. The WPI system was modified from a GDI system and deionized water was pressurized to 50 bar by compressed nitrogen through a high pressure water tank. The effects of WPI on engine power output, combustion phases, knock related indexes and emissions were investigated at two WPI timings of 170 and 360 °CAD BTDC. The water/gasoline volume percentage was varied from 0% to 50%. The main results of this study are summarized as follows:

(1) WPI reduced the intake air temperature and increased the volumetric efficiency. At the original KLSA condition, WPI reduced the combustion rate, slowed the flame kernel formation process (CA0-5) and prolonged the initiation combustion period (CA0-10), leading to reduced combustion stability (higher COV_{IMEP}). As a result, IMEP and engine thermal efficiency were decreased, and specific fuel consumption rate was increased. These adverse effects increase with the increase of water/gasoline percentage.

(2) When WPI was applied, advancing spark timing accelerated the combustion rate (CA50) and shortened the combustion durations (CA0-10 and CA0-90). It also generated higher peak in-cylinder pressure (P_{max}) and IMEP without the occurrence of knock. Compared to non-WPI condition, engine thermal efficiency was increased by 1.5% and fuel consumption was reduced by 10 g/kWh by WPI.

(3) WPI effectively reduced the combustion temperature and suppressed engine knock. The spark timing of WPI condition could be further increased than non-WPI condition, leading to faster combustion rate and higher thermal efficiency. However, excessive water/gasoline percentage had adverse effect on engine performance. When it exceeded a certain percentage (30% in this study), the engine power output could not be restored by adjusting spark advance.

(4) WPI resulted in more incomplete combustion and higher ISHC. On the other hand, ISNO was significantly reduced due to the reduction in combustion temperature. FSN emissions were significantly reduced when water/gasoline percentage was within 30%. The water/gasoline percentage of 30% was the optimum ratio in this test where the engine efficiency was improved and emissions could maintained at low level.

References

[1] Fraser N, Blaxill H, Lumsden G, et al. Challenges for increased efficiency through gasoline engine downsizing. SAE International Journal of Engines, 2009, 2(1): 991-1008.

[2] Huang Y, Hong G. Investigation of the effect of heated ethanol fuel on combustion and emissions of an ethanol direct injection plus gasoline port injection (EDI+ GPI) engine. Energy Conversion and Management, 2016, 123: 338-347.

[3] Hopkinson B. A New Method of Cooling Gas-Engines. Journal of the Royal Society of Arts.

1913;61(3168):867-72.

[4] Ricardo BHR. The high-speed internal-combustion engine1953.

[5] Battistoni M, Grimaldi C N, Cruccolini V, et al. Assessment of port water injection strategies to control knock in a GDI engine through multi-cycle CFD simulations. SAE Technical Paper, 2017.

[6] Morsy M H. Assessment of a direct injection diesel engine fumigated with ethanol/water mixtures. Energy conversion and management, 2015, 94: 406-414.

[7] Zhu S, Hu B, Akehurst S, et al. A review of water injection applied on the internal combustion engine. Energy conversion and management, 2019, 184: 139-158.

[8] Arabaci E, İçingür Y, Solmaz H, et al. Experimental investigation of the effects of direct water injection parameters on engine performance in a six-stroke engine. Energy conversion and management, 2015, 98: 89-97.

[9] Chintala V, Subramanian K A. Experimental investigation of hydrogen energy share improvement in a compression ignition engine using water injection and compression ratio reduction. Energy conversion and management, 2016, 108: 106-119.

[10] Boretti A. Water injection in directly injected turbocharged spark ignition engines. Applied Thermal Engineering, 2013, 52(1): 62-68.

[11] Hermann I, Glahn C, Kluin M, et al. Water Injection for Gasoline Engines: Quo Vadis [C]//International Conference on Knocking in Gasoline Engines. Springer, Cham, 2017: 299-321.

[12] TSZHO. Elite master BMW M4 Coupe Competiton Edition. Car test report. 2017(1):137-9.

[13] Brusca S, Galvagno A, Lanzafame R, et al. Fuels with low octane number: water injection as knock control method. Heliyon, 2019, 5(2): e01259.

[14] Lestz S S, Meyer W E. The Effect of Direct Cylinder Water Injection on Nitric Oxide Emission from an SI Engine[C]//Proceedings of the 14th FISITA Congress. 1972: 2134-2141.

[15] Daniel R, Wang C, Xu H, et al. Dual-injection as a knock mitigation strategy using pure ethanol and methanol. SAE International Journal of Fuels and Lubricants, 2012, 5(2): 772-784.

[16] Wei L, Yao C, Han G, et al. Effects of methanol to diesel ratio and diesel injection timing on combustion, performance and emissions of a methanol port premixed diesel engine. Energy, 2016, 95: 223-232.

[17] Huang Y, Hong G, Huang R. Numerical investigation to the dual-fuel spray combustion process in an ethanol direct injection plus gasoline port injection (EDI+ GPI) engine. Energy conversion and management, 2015, 92: 275-286.

[18] Hoppe F, Thewes M, Baumgarten H, et al. Water injection for gasoline engines: Potentials, challenges, and solutions. International Journal of Engine Research, 2016, 17(1): 86-96.

[19] Zhuang Y, Qian Y, Hong G. Lean Burn Performance of a Spark Ignition Engine with an Ethanol–Gasoline Dual Injection System. Energy & fuels, 2018, 32(3): 2855-2868.

[20] Worm J, Naber J, Duncan J, et al. Water injection as an enabler for increased efficiency at high-load in a direct injected, boosted, SI engine. SAE International Journal of Engines, 2017, 10(3): 951-958.

[21] Fu L, Wu Z, Yu X, et al. Experimental investigation of combustion and emission characteristics for internal combustion rankine cycle engine under different water injection laws. Energy Procedia, 2015, 66: 89-92.

[22] Wang C, Zhang F, Wang E, et al. Experimental study on knock suppression of spark-ignition engine fuelled with kerosene via water injection. Applied energy, 2019, 242: 248-259.

[23] Qiang S, Ji-Guang Y. Effect of water injection phasing on combustion process in ICRC engine. 2014.

[24] Gadallah A H, Elshenawy E A, Elzahaby A M, et al. Effect of in cylinder water injection strategies on perfomance and emissions of a hydrogen fuelled direct injection engine. SAE Technical Paper, 2009.

[25] Bhagat M, Cung K, Johnson J, et al. Experimental and numerical study of water spray injection at engine-relevant conditions. SAE Technical Paper, 2013.

[26] d'Adamo A, Berni F, Breda S, et al. A Numerical Investigation on the Potentials of Water Injection as a Fuel Efficiency Enhancer in Highly Downsized GDI Engines. SAE Technical Paper, 2015.

[27] Rohit A, Satpathy S, Choi J, et al. Literature survey of water injection benefits on boosted spark ignited engines. SAE Technical Paper, 2017.

[28] Breda S, Berni F, d'Adamo A, et al. Effects on knock intensity and specific fuel consumption of port water/methanol injection in a turbocharged GDI engine: Comparative analysis. Energy Procedia, 2015, 82: 96-102.

[29] Fraser N, Blaxill H, Lumsden G, et al. Challenges for increased efficiency through gasoline engine downsizing. SAE International Journal of Engines, 2009, 2(1): 991-1008.

[30] Huang Y, Hong G. Investigation of the effect of heated ethanol fuel on combustion and emissions of an ethanol direct injection plus gasoline port injection (EDI+ GPI) engine. Energy Conversion and Management, 2016, 123: 338-347.

[31] Valero-Marco J, Lehrheuer B, López J J, et al. Potential of water direct injection in a CAI/HCCI gasoline engine to extend the operating range towards higher loads. Fuel, 2018, 231: 317-327.

[32] Liu F, Consalvi J L, Fuentes A. Effects of water vapor addition to the air stream on soot formation and flame properties in a laminar coflow ethylene/air diffusion flame. Combustion and Flame, 2014, 161(7): 1724-1734.

[33] Nande A M, Wallner T, Naber J. Influence of water injection on performance and emissions of a direct-injection hydrogen research engine. SAE Technical Paper, 2008.

[34] Huang Z H, Pan K Y, Zhou L B, et al. Effect of top land width and engine operating conditions on exhaust hydrocarbon emissions from a spark ignition engine[J]. Proceedings of the Institution of Mechanical Engineers, Part D: Journal of Automobile Engineering, 1996, 210(3): 243-247.

[35] Huang Z, Pang J, Pan K, et al. Investigation into hydrocarbon emissions from crevice and oil film during cold start and idling periods in a spark ignition engine[J]. Proceedings of the Institution of Mechanical Engineers, Part D: Journal of Automobile Engineering, 1998, 212(6): 501-505.

[36] Zhang Y, Huang Z, Wei L, et al. Experimental and modeling study on ignition delays of lean mixtures of methane, hydrogen, oxygen, and argon at elevated pressures[J]. Combustion and Flame, 2012, 159(3): 918-931.

[37] Tang C, Man X, Wei L, et al. Further study on the ignition delay times of propane–hydrogen–oxygen–argon mixtures: Effect of equivalence ratio[J]. Combustion and Flame, 2013, 160(11): 2283-2290.